Complementary Perturbation of the Kinetic Mechanism and Catalytic Effectiveness of Dihydrofolate Reductase by Side-Chain Interchange†

Carston R. Wagner,‡ Joelle Thillet,§ and Stephen J. Benkovic*

Department of Chemistry, 152 Davey Laboratory, The Pennsylvania State University, University Park, Pennsylvania 16802

Received March 13, 1992; Revised Manuscript Received May 14, 1992

ABSTRACT: The variable residue Leu-28 of *Escherichia coli* dihydrofolate reductase (DHFR) and the corresponding residue Phe-31 in murine DHFR were interchanged, and the impact on catalysis was evaluated by steady-state and pre-steady-state analysis. The *E. coli* L28F mutant increased the pH-independent k_{cat} from 11 to 50 s^{-1} but had little effect on $K_m(H_2F)$. An increase in the rate constant for dissociation of H_4F from $E{\cdot}H_4F{\cdot}NH$ (from 12 to 80 s^{-1}) was found to be largely responsible for the increase in k_{cat}. Unexpectedly, the rate constant for hydride transfer increased from 950 to 4000 s^{-1} with little perturbation of NADPH and $NADP^+$ binding to E. Consequently, the flux efficiency of the *E. coli* L28F mutant rose from 15% to 48% and suggests a role in genetic selection for this variable side chain. The murine F31L mutant decreased the pH-independent k_{cat} from 28 to 4.8 s^{-1} but had little effect on $K_m(H_2F)$. A decrease in the rate constant for dissociation of H_4F from $E{\cdot}H_4F{\cdot}NH$ (from 40 to 22 s^{-1}) and $E{\cdot}H_4F$ (from 15 to 0.4 s^{-1}) was found to be mainly responsible for the decrease in k_{cat}. The rate constant for hydride transfer decreased from 9000 to 5000 s^{-1} with minor perturbation of NADPH binding. Thus, the free energy differences along the kinetic pathway were generally similar in magnitude but opposite in direction to those incurred by the *E. coli* L28F mutant. This conclusion implies that DHFR hydrophobic active-site side chains impart their characteristics individually and not collectively.

The design of catalysts that will retain their original catalytic activity and efficacy on totally unnatural substrates is an expressed objective of protein engineering. To approach this challenge, one needs to understand the impact that point-site as well as substructural changes can have on the catalytic process. Recent evidence from site-directed mutagenesis and crystallographic studies of mutant enzymes implies that the overall protein structure can often accommodate the imposed substitution (Johnson & Benkovic, 1991). Realizing the utility of this conclusion, Clarke et al. (1989) were able to shift the substrate specificity of lactate dehydrogenase (LDH) from pyruvate to oxaloacetate by the replacement of a variable glutamine in the active site with arginine. Comparison of the structural and sequence data for LDH with malate dehydrogenase (MDH) had suggested that the mutated active site would be better able to satisfy the additional substrate carboxylate of the pseudosubstrate. Consequently, the active-site surfaces of LDH and MDH can be viewed as an assembly of independent modules in which side chains can be exchanged, transferring their effects from one surface to the other. We chose to explore the generality of this conclusion by examining the interchange of a variable hydrophobic contact described by the X-ray crystallographic data for the active site of dihydrofolate reductase.

Dihydrofolate reductases isolated from bacterial and mammalian sources manifest differing substrate specificities for the NADPH-dependent reduction of 7,8-dihydrofolate (H_2F)[1] and folate. For example, the murine enzyme at pH 6.0 reduces folate 1000 times faster than the *Escherichia coli* enzyme. The pH-independent rate coefficient of hydride transfer for murine DHFR is 10-fold greater than that for *E. coli* DHFR, whereas the rate constant for H_4F product dissociation from $E{\cdot}NH{\cdot}H_4F$ rises from 12 to 40 s^{-1}. Sequence alignment of known DHFRs from various sources reveals several strictly conserved residues within the active site. Site-directed mutagenesis experiments have demonstrated that several of these residues lining the binding cleft for H_2F as well as NADPH are critically important for (1) maximizing enzyme efficacy at neutral pH, (2) binding and release of substrates and products, and (3) lowering the free energy barrier for hydride transfer.

Despite virtually superimposable tertiary structures for *E. coli*, *Lactobacillus casei*, avian, and murine DHFRs, the extent of active-site homology, unlike LDH and MDH, is at most 50% (Naylor, personal communication), implying that the active-site surface can withstand an exceptional amount of variation. Examination of the *E. coli* DHFR folate binding site reveals four potentially important hydrophobic contacts (Figure 1): Leu-28, Phe-31, Ile-50, and Leu-54. Conserved residues 31 and 54 are known to contribute as much as 2.0 kcal/mol in the binding of H_2F and between 1.0 and 2.5 kcal/mol toward the stabilization of the hydride-transfer step (Mayer et al., 1986; Chen et al., 1987; Murphy & Benkovic, 1989). In contrast, the side chain at position 28 exhibits species variation. For example, Leu-28 of *E. coli* aligns with Phe-31 in mouse DHFR and Tyr-31 in avian DHFR, respectively.

Recently the complete kinetic mechanisms for the *E. coli* (Fierke et al., 1987a), *L. casei* (Andrews et al., 1989), and

† Supported by NIH Grant GM24129. C.R.W. was an NIH Postdoctoral Fellow.

* To whom correspondence should be addressed.

‡ Present address: Department of Medicinal Chemistry, College of Pharmacy, University of Minnesota, Minneapolis, MN 55455.

§ Visiting Scientist from Unite 257 de Institut National de la Sante et de la Recherche Medicale, Institut Jacques Monod du Centre National de la Recherche Scientifique, Tour 43-2 Place Jussieu, 75005 Paris, France.

[1] Abbreviations: $^DV = {}^Dk_{cat}/{}^Hk_{cat}$; DHFR, dihydrofolate reductase; DTT, dithiothreitol; H_2F, dihydrofolate; H_4F, tetrahydrofolate; LM, Luria–Bertani medium with added Mg^{2+}; MES, 2-(*N*-morpholino)-ethanesulfonic acid monohydrate; MTX, methotrexate; Tris, tris(hydroxymethyl)aminomethane; NH, NADPH; N, $NADP^+$.

0006-2960/92/0431-7834$03.00/0

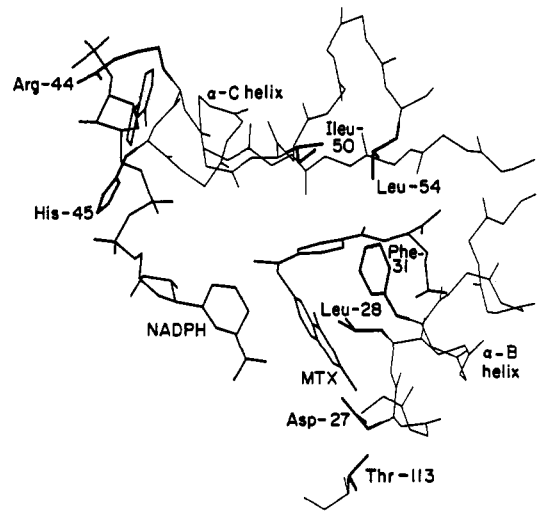

FIGURE 1: Active site of *E. coli* DHFR. The α-C and α-B helices are shown with respect to NADPH and MTX (Bolin et al., 1982).

murine (Thillet et al., 1990) DHFRs have been elucidated. Within the confines of the kinetic boundaries for the various DHFRs, the contributions of the active-site surface topography to binding and catalysis are addressable. If side-chain variations perturb the kinetic mechanism, are they independent of or dependent on remote or local sequence variation? To answer this question, site-directed mutagenesis was employed to interchange the residue at position 28 of *E. coli* DHFR with that for murine DHFR (Leu to Phe), and, reciprocally, the residue at position 31 of murine DHFR was switched with that for *E. coli* DHFR (Phe to Leu). Steady-state and pre-steady-state parameters for the mutant and wild-type enzymes were then compared.

MATERIALS AND METHODS

Substrates and Buffers. 7,8-Dihydrofolate (H_2F) was prepared by the dithionite reduction of folic acid (Blakley, 1960), and (6*S*)-tetrahydrofolate was prepared from H_2F by enzymatic conversion with DHFR (Mathews & Huennekens, 1960). Purification was achieved on a DE-54 resin with a linear triethylammonium bicarbonate gradient (Curthoys et al., 1972). NADPH, $NADP^+$, MTX, and folic acid were purchased from Sigma.

2,4-Diamino-6,7-dimethylpteridine (DAM) was purchased from ICN Pharmaceuticals. [4′(*R*)-^{2}H]NADPH (NADPD) was prepared (Stone & Morrison, 1982) by using *Leuconostic mesenteroides* alcohol dehydrogenase purchased from Research Plus Inc., and purified by the method of Viola et al. (1979). Excess NaCl was removed from the purified NADPD by a Biogel P-2 desalting column (Howell et al., 1987). Ligand concentrations were determined spectrophotometrically by using the following extinction coefficients: H_4F, 28 000 M^{-1} at 297 nm, pH 7.5 (Kallen & Jencks, 1966); H_2F, 28 000 M^{-1} at 282 nm, pH 7.4 (Dawson et al., 1969); folic acid, 27 600 M^{-1} at 282 nm, pH 7.0 (Rabinowitz 1960); MTX, 22 100 M^{-1} at 302 nm in 0.1 N KOH (Seeger et al., 1949); NADPH, 6200 M^{-1} at 339 nm, pH 7.0; $NADP^+$, 18 000 M^{-1} at 259 nm, pH 7.0. The concentrations of H_2F and NADPH were also determined by DHFR turnover.

All kinetic measurements were obtained at 25 °C in buffer containing 50 mM 2-(*N*-morpholino)ethanesulfonic acid (MES), 25 mM tris(hydroxymethyl)aminomethane (Tris), 25 mM ethanolamine, and 100 mM sodium chloride (MTEN buffer, pH 5–10) or 25 mM MES, 50 mM Tris, 25 mM sodium acetate, and 100 mM sodium chloride (MTAN buffer, pH 4–5) (Ellis & Morrison, 1982). Extensively degassed and argon-purged buffers were used in the presence of H_4F.

E. coli Strains and Biochemicals. The following strains were obtained as a gift from P. Stanssens: BMH-71 (*mutS*215: *Tn*10), W71-18 (*su*-:*hpsl*), and MK30-3 (*rec* A$^-$, *su*$^-$). JM-109 was obtained from A. Onishi and maintained on minimal media. DH5-α (Strategene) was purchased from BRL/Gibco Inc. Unless otherwise noted, all transformations were carried out according to the method of Hanahan (1983). M13K07 helper phage was obtained from Pharmacia Inc.

Ultrapure agarose was purchased from FMC Inc. The enzymes T4 DNA ligase and T4 polynucleotide kinase were purchased from Boehringer Mannheim. Restriction endonucleases *Aat*II, *Bam*HI, *Sma*I, *Cla*I, *Nar*I, *Eag*I, and *Dra*I were purchased from New England Biolabs Inc. Calf intestinal phosphatase was purchased from Sigma. *E. coli* DNA polymerase Pol I (Klenow fragment) and T4 polymerase were purified in our laboratory by Bryan Eger and Todd Capson.

Overproduction and Oligonucleotide-Directed Mutagenesis. From the plasmid pTZ-74 obtained as a gift from M. Iwakura, a 1100 bp DNA fragment flanked by two *Aat*II restriction sites containing the *fol* gene and tac promoter was excised and isolated by agarose gel electrophoresis onto activated nitrocellulose paper. The fragment was blunt-ended with T4 polymerase and ligated with T4 ligase to *Bam*HI linkers obtained from New England Biolabs. Concurrently, the mutagenenic pMa/c-type plasmids pMa-5 and pMc-5 were obtained as a gift from P. Stanssens. pMa-5, which contains a *Bam*HI restriction site within its cloning cartridge, was digested, dephosphorylated with calf intestinal phosphatase, purified by agarose gel electrophoresis, and isolated on activated nitrocellulose paper.

After digestion with *Bam*HI and purification, the *fol* fragment was ligated to the *Bam*HI-digested pMa-5 to produce pRWa-1. Ligation polarity was confirmed by a double digest with *Eco*RI and *Hin*dIII. Upon transformation of either W71-18 or MK30-3 with pRWa-1, 15–20% of the total cellular protein, when analyzed by gel electrophoresis of cell lysates, was expressed as DHFR. The resulting plasmid, pRWa-1, allowed mutagenesis and overproduction to be carried out by the same vector.

Oligonucleotide-Directed Mutagenesis. Mutagenesis at position 28 in *E. coli* was carried out as described by Stanssens et al. (1989). The mutagenenic oligonucleotide [GCCT-GCCGATTTCGCCTGG (L28F)] was obtained from and HPLC-purified by the Penn State Biotechnology oligonucleotide synthesis facility. Single-stranded pRWa-1 was obtained by inoculating cultures of JM-109 previously transformed by pRWa-1 with the helper phage M13KO7. After purification of the ss pRWa-1 by standard procedures (Maniatis et al., 1982), gapped duplex DNA was constructed by annealing linearized pMc-5 (digested by *Cla*I and *Sma*I) to ss pRWa-1. The construct covered the promoter but left the *fol* gene exposed for mutagenesis. The gapped duplex was filled by first annealing the mutagenic oligonucleotide of choice to the gapped duplex followed by treatment with *E. coli* DNA polymerase Pol I (Klenow fragment) and T4 DNA ligase. The repair deficient *E. coli* strain BMH-71 *mut S* was transformed with the gapped-filled DNA and grown overnight in LM. After isolation and purification of the mutant plasmid DNA by the method of Birnboim and Doly (1979), segregation of the wild type from mutant genes was accomplished by transformation of W71-18 *su*- or MK30-3 *su*- with the isolated DNA, followed by plating onto LM/ampicillin (100 μg/mL). Candidates for the L28F mutant were screened

by colony hybridization with the ^{32}P-labeled mutagenic oligonucleotide. Mutant DNA was then fully sequenced by the method of Sanger et al. (1977), thus assuring that no additional mutations had been incorporated. Mutagenic efficiencies ranged from 30 to 95%.

The murine F31L mutant was prepared by oligonucleotide-directed mutagenesis and the mutant DNA transferred to an expression vector as previously described (Thillet et al., 1988).

Protein Purification. Strain MK30-3 was transformed with the plasmid for the *E. coli* L28F mutant. Single colonies were selected and grown in small culture [10 mL of LB, ampicillin (100 μg/mL), and trimethoprim (20 μg/mL)] to an OD_{600} = 1.5 followed by dilution into 1 L of LB [ampicillin (100 μg/mL)] and grown to the same OD. The cells were collected by centrifugation, and protein purification was carried out as described by Baccanari et al. (1977) and Chen et al. (1987), routinely yielding 8–10 mg of protein/g of cells. The purification of the mouse F31L mutant was performed as previously described (Thillet et al., 1988).

Steady-State Kinetics. Initial velocities for the enzyme reactions were measured by using either a Gilford 240 or a Cary 219 UV–visible spectrophotometer at 25 °C. The molar absorbance change used was 11 800 M^{-1} (Stone & Morrison, 1982). DHFR was preincubated with varying amounts of NADPH before H_2F was added to remove hysteretic effects (Penner & Frieden, 1985). The intrinsic pK_a of the enzymes was determined from DAM inhibition studies previously described by Stone and Morrison (1983).

Fluorescence Titrations. The thermodynamic dissociation constants (K_d) for ligand binding to the mutant DHFRs were measured by fluorescence titration at 25 °C on an SLM 8000 spectrofluorometer. Quenching of the intrinsic enzyme fluorescence at 340 nm upon excitation at 290 nm was monitored as a function of ligand concentration (Birdsall et al., 1980; Stone & Morrison, 1982; Taira & Benkovic, 1988). Standard tryptophan solutions were used to correct for ligand internal filter effects. Usually the enzyme concentration used was either at or slightly less than the K_d of the ligand. The data were fit by a nonlinear least-squares fitting program previously described (Taira & Benkovic, 1988).

Transient Binding and Pre-Steady-State Kinetics. Transient binding and pre-steady-state kinetic experiments were performed on an Applied Photophysics Inc. stopped-flow spectrophotometer capable of absorbance and fluorescence measurements at 25 °C and fitted with a monochromator for generating the excitation input. The instrument has a 1.4-ms dead time with a 2- or 10-mm cell path length from which either fluorescence or transmittance can be observed. In most cases, ligand binding experiments were monitored by excitation of DHFR fluorescence at 290 nm and observation of the degree of quenching at 340 nm by using an output cutoff filter for the range 250–400 nm. Absorbance measurements were monitored at 340 nm using the 250–400-nm cutoff filter. Typically, three to six traces were recorded and averaged for future data analysis.

After the trigger impulse, data were collected by an Archimedies computer over a preselected time range from 5 ms to 15 min. Kinetic data were fit by using a nonlinear least-squares computer program provided by Applied Photophysics Inc. that analyzed the transients as single or double exponentials, or as a single exponential followed by a linear segment. Binding and pre-steady-state data were then transferred to a VAX microcomputer and fit to various mechanisms by using the kinetic simulation program KINSIM (Barshop et al., 1983) modified by K. Johnson and J. Wagner.

Table I: Steady-State Parameters for Wild-Type and Mutant Dihydrofolate Reductases

parameter	*E. coli*	L28F	mouse[b]	F31L
k_{cat} (s^{-1})[c]	12.3 ± 0.7	50 ± 5	28 ± 2	4.8 ± 0.6
$K_m(H_2F)$ (μM)[c]	0.7 ± 0.2	1.0 ± 0.3	0.9 ± 0.3	0.67 ± 0.2
V/K (μM^{-1} s^{-1})[c]	17.6	55 ± 20	35 ± 14	7.7 ± 2.8
p$K_a(V)$[d]	8.4	8.7 ± 0.1		9.52 ± 0.04
p$K_a(V/K)$[d]	8.1	8.5 ± 0.2		
pK_a	6.5 ± 0.1	6.6 ± 0.2	6.4 ± 0.05	6.6 ± 0.1
^DV	1.0 ± 0.1 (pH 6.0)	0.98 ± 0.1 (pH 6.0)	1.0 ± 0.12 (pH 8.5)	1.1 ± 0.1 (pH 6.0)
^DV	2.7 ± 0.1 (pH 9.0)	3.0 ± 0.2 (pH 9.0)	3.3 ± 0.25 (pH 10.0)	2.6 ± 0.1 (pH 10.0)
V_1 (s^{-1})[c]			17 ± 2	1.2 ± 0.1
K_{m1}(NADPH) (μM)[c]			6.2 ± 1.0	1.9 ± 0.2
V_2 (s^{-1})[c]			36 ± 2	25 ● 2
K_{m2}(NADPH) (μM)[c]			49 ± 4	270 ± 20

[a] Data taken from Fierke et al. (1987a). [b] Data taken from Thillet et al. (1990). [c] pH-independent values. [d] pK_a values were determined under conditions of varying H_2F (1–100 μM) and constant NADPH (100 μM) levels.

RESULTS

Steady-State Kinetic Parameters. The Michaelis–Menten parameters, k_{cat} and K_m, were determined by varying the H_2F concentration (1–80 μM) while holding the NADPH concentration constant (100 μM) (Table I). Varying the NADPH concentration (1–300 μM) at 50 μM H_2F provided linear double-reciprocal plots for the *E. coli* L28F mutant. However, as was demonstrated for the murine DHFR (Thillet et al., 1990), the initial velocity data for the murine F31L mutant under variable coenzyme concentrations (Table I) were best fit by two V's and two K_m's to the following equation: $v = V_1[S]/(K_{m1} + [S]) + V_2[S]/(K_{m2} + [S])$. Neither mutation affected the enzyme's catalytic activity toward folate (data not shown).

As had been shown previously for wild-type *E. coli* (Fierke et al., 1987a), *L. casei* (Andrews et al., 1989), and murine (Thillet et al., 1990) DHFRs, the reaction catalyzed by each mutant (*E. coli* or murine) exhibited a strong pH dependence. In each case, as the pH decreased a constant velocity was reached, implying that maximum velocity is facilitated by the pre-protonation of a residue on the active site. Analysis of the V and V/K profiles in terms of a single pK_a gave satisfactory fits to the observed data, yielding the values shown in Table I. Also included in Table I are the deuterium isotope effects on V (^DV) for the mutants at low and high pH, with saturating [4′(*R*)-^{2}H]NADPH showing a full isotope effect of 2.7–3.0 at high pH.

The reverse rate of the reaction (i.e., net conversion of H_4F and $NADP^+$ to form H_2F and NADPH) for the L28F mutant was measured by monitoring the increase in absorbance at 340 nm in a reaction mixture containing 200 μM H_4F, 2 mM $NADP^+$, 0.1 M NaCl, and 3 mM DTT in degassed MTEN buffer, pH 10.0 at 25 °C (Table III). Neither doubling the substrate concentration nor decreasing the buffer pH to 9.0 had any effect on the observed rate of these reactions. The reverse rate for the F31L murine mutant was measured by pre-steady-state methods (vide infra).

Binding Kinetics by a Relaxation Method. Stopped-flow quenching of the intrinsic enzyme fluorescence has been used to measure the association and dissociation rate constants of ligand to several wild-type and mutant DHFRs (Dunn & King, 1978; Cayley et al., 1981; Fierke et al., 1987a; Adams et al., 1989; Fierke & Benkovic, 1989; Murphy & Benkovic, 1989; Appleman et al., 1990; Thillet et al., 1990; Beard et al.,

Table II: Thermodynamic Dissociation Constants, K_d (μM),[a] for Ligands to Mutant and Wild-Type DHFRs

ligand	*E. coli*[c]	L28F	mouse[d]	F31L
NADPH	0.33	0.40 ± 0.05	1.85	1.7 ± 0.2
NADPH[b]	0.42	0.18 ± 0.04	2.0	
$NADP^+$	22		3.71	21.8 ± 6.0
H_2F	0.22	0.15 ± 0.06	0.81	0.019 ± 0.009
H_2F[b]	1.19	1.5 ± 0.2	1.21	

[a] Obtained from fluorescence titration experiments. [b] Calculated from $K_d = (k_{off}/k_{on})[1 + 1/(k_{-2}/k_2)]$ (Fierke et al., 1987a). [c] Data from Fierke et al. (1987a). [d] Data from Thillet et al. (1990).

Scheme I

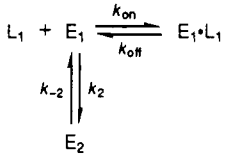

1991). During the formation of binary complexes of DHFR, the observed rate constant (k_{obs}) increases linearly with ligand concentration when [L] > [E]. Under these pseudo-first-order reaction conditions, $k_{obs} = k_{on}[L] + k_{off}$ where k_{on} and k_{off} are the association and dissociation rate constants, respectively. Thus, a linear plot of k_{obs} versus [L] yields k_{on} from the slope and k_{off} from the k_{obs} intercept. The association and dissociation rate constants for cofactor and L28F were 23.8 ± 0.99 μM^{-1} s^{-1} and 2 ± 1 s^{-1}, which are similar to the values of 20 μM^{-1} s^{-1} and 3.5 s^{-1} for wild type, respectively. Substrate binding exhibited roughly a 2-fold increase to 105 ± 10 μM^{-1} s^{-1} and 93 ± 15 s^{-1} in both the association and dissociation rate constants, respectively. Unfortunately, the extent of fluorescence quenching was inadequate to permit similar binding experiments with the F31L murine mutant.

At saturating NADPH levels, the ligand-dependent phase used to measure k_{obs} is followed by a ligand-independent phase (Cayley et al., 1981). This observation is consistent with the slower isomerization of a second enzyme form, E_2, to the ligand binding conformer, E_1 (Scheme I). The rate constant for interconversion of E_2 to E_1 (k_{-2}) can be obtained from the second phase, and the equilibrium constant (K_{eq}) is determined from the ratio of the amplitudes of the fast and slow phases. The L28F mutant exhibited a rate of E_2 to E_1 conversion of 0.042 ± 0.005 s^{-1} and an E_1/E_2 ratio of 1.3 ± 0.1, respectively. These data are close to the values of 0.034 s^{-1} and 0.72 observed for the wild type. No additional ligand-dependent phase was seen with the L28F mutant as noted for wild-type *E. coli* DHFR (Adams et al., 1989).

The K_d for NADPH is related to k_{on} and k_{off} by eq 1. The predicted (from k_{on} and k_{off}) and measured thermodynamic equilibrium dissociation constants for the mutant DHFRs are

$$K_d = k_{off}/k_{on}(1 + 1/K_{eq}) \quad (1)$$

exhibited in Table II. Agreement between these two data sets supports Scheme I for NADPH binding. In contrast, as was observed for all wild-type DHFRs, the binding of H_2F does not fit the above criterion. This has been interpreted as the result of H_2F binding to both E_1 and E_2 conformers (Dunn & King, 1978; Fierke et al., 1987a).

Dissociation Rate Constants by Competition. The dissociation rate constants of ligands from several wild-type and mutant DHFRs can also be measured by the method of competition (Dunn & King, 1978; Fierke et al., 1987a). A preequilibrated enzyme–ligand complex (E·L) is mixed with a large excess of a second trapping ligand (T) which competes for the same binding site. The observed fluorescence change indicates the release of L from the enzyme complex, E·L, and formation of the new complex, E·T, as described in Scheme II. When $k_{on}[L] \ll k_T[T] \gg k_{off}$ and $k_T[T]/k_{-T} \gg k_{on}[L]/k_{off}$, k_{obs} is equal to the dissociation rate constant for L, k_{off}. This measurement was verified by demonstrating that k_{obs} was independent of the concentration of L and T. The dissociation rate constants for several ligand from both binary and ternary complexes of the mutant DHFRs are shown in Table III.

Scheme II

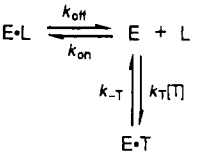

Table III: Dissociation Rate Constants (s^{-1}) of Ligands and Rates of Hydride Transfer in the Reverse and Forward Directions from Mutant and Wild-Type Enzymes

ligand	complex	*E. coli*[a]	L28F	mouse[b]	F31L
NADPH	E	3.5	2.5 ± 0.5	2.8	
	E·H_4F	85	8.0 ± 1.5	26	
$NADP^+$	E	295	157 ± 5	90	
	E·H_4F	200	287 ± 54	440	450 ± 50
H_2F	E	22	90 ± 10	20	
H_4F	E	1.4	40 ± 2	15	0.38 ± 0.01
	E·NH	12	80 ± 5	40	22.1 ± 1.0
	E·N	2.4	34 ± 3	20	
k_H		950	4000 ± 1000	9000	5000 ± 1000
k_{-H}		0.60	0.56 ± 0.06	90	181 ± 13
K_{int}		1600	7000	100	30

[a] Data taken from Fierke et al. (1987a). [b] Data taken from Thillet et al. (1990).

Thermodynamic Dissociation Constants (K_d). The binding of H_2F and NADPH to free DHFR was examined by following the decrease in enzyme fluorescence that occurs upon formation of DHFR-ligand complexes (Taira & Benkovic, 1988). The K_d values for H_2F and NADPH are given in Table II for the mutant enzymes. Generally, changes observed in the K_d's for the L28F and F31L mutants were within an order of magnitude. The F31L K_d for H_2F was an exception, since it is 40-fold lower than that observed for wild type.

Pre-Steady-State Kinetics. The rate constants for hydride transfer from NADPH to H_2F given in Table III were measured from pre-steady-state transients. A rapid burst of product formation was observed by monitoring changes in either absorbance or fluorescence energy transfer as for the wild-type enzymes (Fierke et al., 1987a; Thillet et al., 1990). Typically, the mutant DHFRs were preincubated in 200 μM NADPH or NADPD and diluted 2-fold into 180 μM H_2F to initiate the reaction. From a comparison of the NADPH and NADPD data, an isotope effect on the burst rate constant could be determined after computer fitting the data to a single-exponential decay followed by a linear rate process.

Additionally, the observed rate constants for hydride transfer (k_{for}) were estimated by using the computer simulation program KINSIM (Barshop et al., 1983) to model the data according to Scheme III, incorporating the independently determined rate constants to provide the best fit. Dissociation rate constants used for the simulation of Scheme III for the *E. coli* L28F mutant and murine F31L mutant are listed in Table III. In the absence of directly determined association and dissociation rate constants for H_2F binding to the F31L

Scheme III

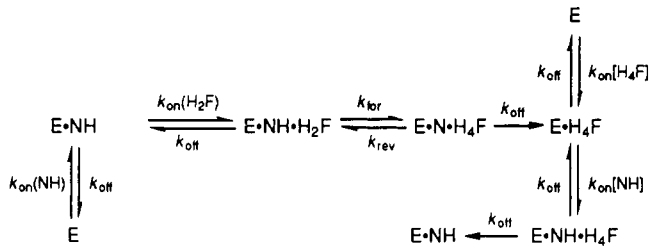

mutant, values were estimated from K_m to be 30 μM^{-1} s^{-1} and 12 s^{-1} and for NADPH binding to the E·H_4F complex from K_{m2} to be 1 μM^{-1} s^{-1} and 260 s^{-1}. The rate constants for association of H_4F to E (25 μM^{-1} s^{-1} for L28F and 33 μM^{-1} s^{-1} for F31L) and for the binding and dissociation of NADPH to E for F31L were assumed equivalent to wild type. The binding of H_2F to E·NH was set equal to values measured for binding of H_2F to E. The simulation was consistent with a single-phase pre-steady-burst for each mutant that corresponded to 0.8 ± 0.1 enzyme equiv.

In order to determine the rate constant for hydride transfer from the protonated ternary complex (H·E·NH·H_2F) and the intrinsic pK_a of the complex, the pH dependence of the observed hydride-transfer rate constant (k_{for}) was measured. The data were then fit to eq 2, yielding the intrinsic pK_a and the pH-

$$k_{for} = k_H/(1 + K_a/[H^+]) \quad (2)$$

independent hydride-transfer rate constant (k_H). Because the burst rates at low pH exceeded the detection limits of the stopped-flow instrument for the L28F and F31L mutants, the pK_a determined by DAM titration (Stone & Morrison, 1983) was used to calculate the pH-independent hydride-transfer rates.

Unlike the *E. coli* mutant DHFRs, the rate of hydride transfer in the reverse direction (k_{rev}) for the murine F31L mutant was characterized by a burst of NADPH formation followed by a linear rate process (Table III) reflecting the slow dissociation of NADPH or H_2F from the enzyme. Typically, 10 μM enzyme was preequilibrated with 2.0 mM $NADP^+$ followed by rapid mixing with 1.0 mM H_4F at pH 10. The data were then fit to a single exponential followed by a linear process. Since decreasing the pH to 9.0 or increasing the concentration of $NADP^+$ had no effect on the burst or linear phase, the measured transient was a pH maximum and was not limited by $NADP^+$ binding, so that k_{rev} is k_{-H}, the rate constant for hydride transfer in the reverse direction.

DISCUSSION

Recently, X-ray crystallographic studies were completed for various binary and ternary ligand complexes of *E. coli* DHFR (Bolin et al., 1982; Filman et al., 1982; Bystroff et al., 1990; Bystroff & Kraut, 1991). The folate binding site is composed of four hydrophobic side chains: (1) Leu-28 and Phe-31 which reside on the α-C helix; (2) Ile-50 which is placed at the end of the α-C helix; and (3) Leu-54 which resides on the hairpin turn that connects the α-C helix and the β-C strand (Figure 1). Residues F-31 and L-54 are strictly conserved across all known DHFR sequences while a significant amount of amino acid variation is well tolerated at positions 28 and 50.

The complete kinetic mechanisms for *E. coli* and murine DHFRs have been elucidated and shown to contain the following key features: (1) H_4F release limits steady-state turnover at neutral pH; (2) the preferred pathway for H_4F release is from the mixed ternary E·NH·H_4F complex; and (3) the overall reaction strongly favors H_4F formation, also reflected in the high value associated with the internal equilibrium (K_{int} = 100–1000) for the reactive ternary complexes. Overall turnover differs from one species to another because of variance in the rates of individual steps. For example, the pH-independent rate of hydride transfer for murine DHFR is 10-fold greater than that for *E. coli* DHFR, whereas the rate of H_4F dissociation from the E·NH·H_4F complex increases 3-fold to 40 s^{-1}.

Within this structural and mechanistic framework, the impact of point-site and substructural changes on the catalytic effectiveness of *E. coli* and murine DHFRs can be evaluated. For example, previous experiments have demonstrated the importance of Phe-31 and Leu-54 in binding and catalysis (Chen et al., 1985; Murphy & Benkovic, 1989). To access the significance of hydrophobic side-chain variation at position 28 on the catalytic effectiveness of DHFR, and in particular the influence of their active-site environment, two point-site mutations were constructed in which the active-site side chains of the *E. coli* and murine enzymes were interchanged and their kinetics evaluated.

E. coli to Mouse Switch. Murine DHFR differs from the *E. coli* enzyme by the substitution of a phenylalanine for leucine at position 28. Construction of the L28F mutant in *E. coli* DHFR increased the pH-independent k_{cat} 4.2-fold to 50 s^{-1}, mirroring the increased turnover number observed for the murine enzyme (Table I). The jump in k_{cat} for L28F was not reflected in the $K_m(H_2F)$ but was due in part to a 6.6-fold increase in the off rate constant for H_4F from the E·H_4F·NH complex. These results also are consistent with the detected rise from 22 to 90 s^{-1} in the off rate of H_2F from E·H_2F (Table III). Since the association rate constant for H_2F with free enzyme was increased 2-fold, the $K_d(H_2F)$ is little changed from wild-type enzymes (Table II). Determination of k_{cat} and K_m at varying NADPH concentrations with a fixed H_2F concentration at neutral pH revealed little change in the K_m(NH) relative to wild type and provided the same k_{cat} observed under varying H_2F and fixed NADPH conditions. This, coupled with the absence of any significant changes in the binding of NADPH or $NADP^+$ to free enzyme, argues for relatively localized perturbations of the folate binding site by this residue substitution. Although the synergistic enhancement of NADPH dissociation from the E·H_4F·NH complex is decreased by almost an order of magnitude, this decrease parallels the 7-fold lower dissociation rate of H_4F from E·H_4F·NH in the wild type relative to the L28F mutant. Consequently, perturbation of the folate and not the cofactor binding site is probably responsible for changes in H_4F binding. The marginal increase in $NADP^+$ dissociation from the E·H_4F·N complex is in agreement with this conclusion.

Because all previous side-chain substitutions within the active site either have maintained or had a deleterious influence on the catalytic step, it was concluded that, within the constraints of the *E. coli* DHFR active-site surface, the rate of hydride transfer had been maximized by evolution. We did not anticipate that the rate constant for hydride transfer would be 4-fold higher (Table III) than that measured for wild-type *E. coli* DHFR. The data for the L28F mutant apparently in part reflect the 9-fold increase in the rate constant for hydride transfer for the murine DHFR relative to the *E. coli* enzyme. Curiously, the mutation had little impact on k_{-H} even though the value for murine DHFR is 150-fold greater than that for *E. coli* DHFR, suggesting increased ground-

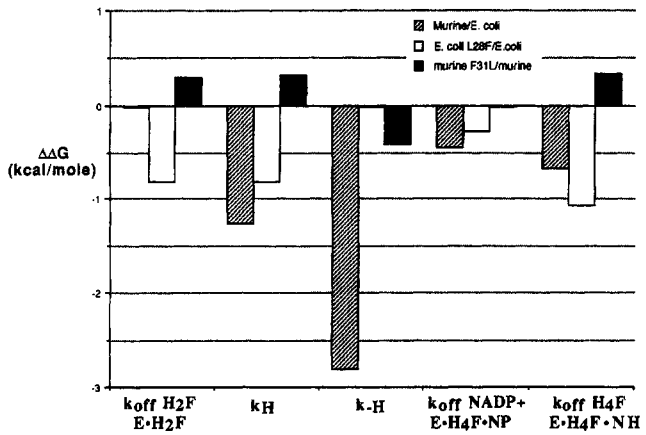

FIGURE 2: Free energy differences between mutant and wild-type DHFRs. $\Delta\Delta G$ values are calculated as follows; e.g., $\Delta\Delta G$ (kcal/mol) for murine/*E. coli* = ΔG for murine − ΔG for *E. coli*.

state ternary product stabilization. From the abbreviated kinetic mechanism described in Scheme III and inputing the appropriate rate constants, the pH-independent k_{cat} is calculated to be 55 s^{-1}, in close agreement with the observed steady-state value of 50 s^{-1}. The apparent pK_a of 8.7 for the L28F mutant is slightly higher than that reported for wild type in response to the parallel increases in the rate for hydride transfer and H_4F dissociation.

By definition, an efficient enzyme mediates a high flux of substrate to product. Maximum catalytic flux is constrained by the diffusion-limited rate constant for substrate binding. In the case of *E. coli* DHFR, the theoretical maximum velocity (v^0_{net}/[E]) is 12 s^{-1}, resulting in a calculated efficiency of 15% under physiological conditions. Previously, active-site mutants of conserved residues have had decreased efficiency by exhibiting negative compensation between an increased product dissociation constant and a decreased rate constant for H_2F association, or hydride transfer. Surprisingly, the *E. coli* L28F mutant displays an efficiency of almost 50% when calculated for physiological conditions (Fierke et al., 1987b). The enhanced efficiency calculated for the substitution at position 28 results primarily from acceleration of H_4F dissociation from the E·H_4F·NH complex, without significant perturbation of the $K_m(H_2F)$.

The changes in the microscopic rate constants when converted to the free energy for L28F compared to the wild-type *E. coli* exhibit the same differences both in magnitude and in direction to those observed when the *E. coli* and the murine enzyme were compared (Figure 2) with the exception of k_{-H}. These data imply that species differences observed in evaluation of the kinetic sequence are in part caused by localized microscopic changes on the active-site surface topography provided by point-site side-chain variability. However, additional compensatory interactions, arising from sequence variation, serve to maintain a similar chemically reactive surface. If this conclusion is warranted, then interchanging Phe-31 with leucine in murine DHFR should produce similar free energy changes, however, opposite in direction.

Mouse to E. coli Switch. To test our hypothesis, Phe-31 in murine DHFR was mutated to leucine. As was mentioned earlier, the wild-type *E. coli* and murine DHFRs are characterized by similar kinetic sequences. At 100 μM NADPH, the pH-independent k_{cat} exhibited a 5.8-fold reduction from 28 to 4.8 s^{-1} with no appreciable perturbation of the $K_m(H_2F)$ or pK_a (Table I). The lack of a kinetic isotope effect in V is in accord with the dissociation of H_4F from E·H_4F·NH remaining rate-limiting despite the decrease in the rate of hydride transfer from 9000 to 5400 s^{-1}. In addition, a 2-fold increase in k_{-H} is indicative of partial ground-state destabilization of the mutant product complex.

Unlike *E. coli* DHFR, the murine enzyme steady-state kinetics are best described by two V's and two K_m's for NADPH owing to the activation by NADPH of H_4F release at higher levels of cofactor (Thillet et al., 1990). This phenomenon was also observed for the murine F31L mutant. The maximal velocities, V_1 and V_2, differed from those for wild type in two crucial respects. First, V_1, which corresponds to the dissociation rate constant for H_4F from E·H_4F, decreased for the murine F31L mutant by greater than 10-fold, while K_{m1}(NH) was reduced only 3-fold. Second, although V_2, which corresponds to the dissociation of H_4F from E·NH·H_4F, only marginally changed, K_{m2}(NH) increased 5.5-fold from 49 to 270 μM, implying a similar increase in the dissociation constant for the binding of NADPH to the binary product complex E·H_4F. The validity of this conclusion was verified by simulating the steady-state parameters using Scheme III and substituting the necessary rate constants. While the dissociation constant for the cofactor to free enzyme was virtually identical to that for wild-type, the murine F31L mutant unexpectedly exhibits decreased (5.5-fold) NADPH binding to the binary product complex, E·H_4F, as derived from the kinetic simulations. A subtle repositioning of bound H_4F and cofactor by the amino acid substitution may explain these perturbations.

Changes in the microscopic rate constants, when converted to differences in free energy for F31L relative to wild-type murine (Figure 2), reveal that the differences are not only of the *same relative magnitude but opposite in direction* to those incurred by the L28F mutation with respect to wild-type *E. coli* DHFR.

CONCLUSIONS

Changes observed for the *E. coli* L28F and murine F31L mutants agree with the effects observed for polar substitutions within the enzyme active site. Instead of being a hopelessly complex array of interdependent interactions, adjustments can be incorporated into the active-site surface with straightforward consequences. The kinetic differences observed between the *E. coli* and murine enzymes are in part due to the singular and independent nature of the contributions of key side chains to the active-site surface through one or more sites of sequence variation. Future examination of active-site double mutants and substructure replacements will more decisively substantiate these assertions.

Hypothetical improvements in enzyme catalytic efficiency have been discussed extensively in terms of defined physiochemical processes (Burbaum et al., 1989). This rationale was applied to DHFR (Fierke et al., 1987b), in conjunction with studies revealing that the free energy changes for mutants of several other enzymes as well as mutants of DHFR are manifest by multiple changes on the ground states and transition states. Potential pathways were identified to improve the enzyme's efficiency to as much as 80%. However, while the necessary kinetic and thermodynamic modifications could be delineated, the molecular route to higher efficiency could not be addressed. Furthermore, given the already high efficiency of the enzyme, possible amino acid substitutions were likely to have a negative impact on efficiency as shown by the deleterious effects of substitutions at the conserved residues 31 and 54. However, the Leu to Phe substitution at position 28 was able to improve substantially the efficiency

of the enzyme, resulting in 300% more substrate being converted to product. Natural selection of the appropriate residue at position 28 is suggested by these data to be critically important for the optimization of DHFR catalytic effectiveness under narrowly defined physiological conditions. Consequently, the organism probably requires a less efficacious or "imperfect" enzyme. Future experiments probing the viability of folate auxotrophs transformed with L28F mutant DNA will answer this question.

ACKNOWLEDGMENT

We thank Drs. Joseph Adams, Carol A. Fierke, Patricia Jennings, Christopher Falzone, and C. Robert Matthews for many informative and helpful discussions. We are particularly grateful to Patricia Benkovic for her thorough reading of the manuscript and to Kaye Yarnell for her expert typing.

REFERENCES

Adams, J., Johnson, K., Matthews, R., & Benkovic, S. J. (1989) *Biochemistry 28*, 6611–6618.

Andrews, J., Fierke, C. A., Birdsall, B., Ostler, G., Feeney, J., Roberts, G. C. K., & Benkovic, S. J. (1989) *Biochemistry 28*, 5743–5750.

Appleman, J. R., Howell, E. E., Kraut, J., & Blakley, R. L. (1990) *J. Biol. Chem. 265*, 5579–5584.

Baccanari, D., Averett, P. D., Briggs, C., & Burchall, J. (1977) *Biochemistry 16*, 3566–3572.

Barshop, B. A. R., Wrenn, F., & Freiden, C. (1983) *Anal. Biochem. 130*, 134–145.

Beard, W. A., Appleman, J. R., Huang, S. M., Delcamp, T. J., Freisheim, J. H., & Blakley, R. L. (1991) *Biochemistry 30*, 1432–1440.

Birdsall, B. A., Burgen, S. V., & Roberts, G. C. K. (1980) *Biochemistry 19*, 3723–3731.

Birnboim, H. C., & Doly, J. (1979) *Nucleic Acids Res. 7*, 1513–1523.

Blakley, R. L. (1960) *Nature (London) 188*, 231–232.

Bolin, J. J., Filman, D. J., Matthews, D. A., Hamlin, R. C., & Kraut, J. (1982) *J. Biol. Chem. 257*, 13650–13662.

Burbaum, J. J., Raines, R. T., Albery, W. J., & Knowles, J. R. (1989) *Biochemistry 28*, 9293–9305.

Bystroff, C., & Kraut, J. (1991) *Biochemistry 30*, 2227–2239.

Bystroff, C., Oatley, S. J., & Kraut, J. (1990) *Biochemistry 29*, 3263–3277.

Cayley, P. J., Dunn, S. M. J., & King, R. W. (1981) *Biochemistry 20*, 874–879.

Chen, J. T., Mayer, R. J., Fierke, C. A., & Benkovic, S. J. (1985) *J. Cell. Biochem. 29*, 73–82.

Chen, J. T., Taira, K., Tu, C. P. D., & Benkovic, S. J. (1987) *Biochemistry 26*, 4093–4100.

Clarke, A. R., Atkinson, T., & Holbrook, J. J. (1989) *Trends Biochem. Sci. 14*, 145–148.

Curthoys, H. P., Scott, J. M., & Rabinowitz, J. C. (1972) *J. Biol. Chem. 247*, 1959–1964.

Dawson, R. M. C., Elliott, D. C., Elliott, W. H., & Jones, K. M. (1969) *Data for Biochemical Research*, Oxford University Press, Oxford.

Dunn, S. M. J., & King, R. W. (1978) *Biochemistry 17*, 766–773.

Ellis, K. J., & Morrison, J. F. (1982) *Methods Enzymol. 87*, 405–426.

Fierke, C. A., & Benkovic, S. J. (1989) *Biochemistry 28*, 478–486.

Fierke, C. A., Johnson, K. A., & Benkovic, S. J. (1987a) *Biochemistry 26*, 4085–4092.

Fierke, C. A., Kuchta, R. D., Johnson, K. A., & Benkovic, S. J. (1987b) *Cold Spring Harbor Symp. Quant. Biol. 52*, 631–638.

Filman, D. J., Bolin, J. T., Matthews, D. A., & Kraut, J. (1982) *J. Biol. Chem. 257*, 13663–13672.

Hanahan, D. (1983) *J. Biol. Chem. 166*, 557–580.

Howell, E. E., Warren, M. S., Booth, C. L. J., Villafranca, J. E., & Kraut, J. (1987) *Biochemistry 26*, 8591–8598.

Johnson, K. A., & Benkovic, S. J. (1991) *The Enzymes* (Sigman, D. S., & Boyer, P. D., Eds.) pp 214–277, Academic Press, San Diego.

Kallen, R. G., & Jencks, W. P. (1966) *J. Biol. Chem. 241*, 5845–5850.

Maniatis, T., Fritsch, E. F., & Sambrook, J. (1982) *Molecular Cloning: a Laboratory Manual*, Cold Spring Harbor Laboratory, Cold Spring Harbor, NY.

Mathews, C. K., & Huennekens, F. M. (1960) *J. Biol. Chem. 235*, 3304–3308.

Mayer, R. J., Chen, J. T., Taira, K., Fierke, C. A., & Benkovic, S. J. (1986) *Proc. Natl. Acad. Sci. U.S.A. 83*, 7718–7720.

Murphy, D. J., & Benkovic, S. J. (1989) *Biochemistry 28*, 3025–3031.

Penner, M. H., & Frieden, C. (1985) *J. Biol. Chem. 260*, 5366–5369.

Rabinowitz, J. C. (1960) *Enzymes, 2nd Ed. 2*, 185–252.

Sanger, F., Nicklen, S., & Coulson, A. R. (1977) *Proc. Natl. Acad. Sci. U.S.A. 74*, 5463–5467.

Seeger, D. R., Cosulick, D. B., Smith, J. M., & Hultquist, M. E. (1949) *J. Am. Chem. Soc. 71*, 1753–1758.

Stanssens, P., Opsomer, C., McKeown, Y. M., Kramer, W., Zabeau, M., & Fritz, H.-J. (1989) *Nucleic Acids Res. 17*, 4441–4454.

Stone, S. R., & Morrison, J. F. (1982) *Biochemistry 21*, 3757–3765.

Stone, S. R., & Morrison, J. F. (1983) *Biochim. Biophys. Acta 745*, 247–258.

Taira, K., & Benkovic, S. J. (1988) *J. Med. Chem. 31*, 129–137.

Thillet, J., Absil, J., Stone, S. R., & Pictet, R. (1988) *J. Biol. Chem. 263*, 12500–12508.

Thillet, J., Adams, J. A., & Benkovic, S. J. (1990) *Biochemistry 29*, 5195–5202.

Viola, R. E., Cook, P. F., & Cleland, W. W. (1979) *Anal. Biochem. 96*, 334–340.